Evaluation of a Rayleigh-Number-Based Freckle Criterion for Pb-Sn Alloys and Ni-Base Superalloys

J.C. RAMIREZ and C. BECKERMANN

A criterion for predicting the formation of freckles for Pb-Sn and Ni-base superalloys is evaluated using available experimental data. The criterion is based on a maximum value of the Rayleigh number, which indicates that the magnitude of buoyancy forces is largest with respect to the retarding frictional forces. The definition of the Rayleigh number involves a characteristic length scale. The two options explored in this study are the distance from the liquid mush interface and the scale represented by the ratio of thermal diffusivity to the casting speed. Additionally, two alternative ways of computing the mushy-zone permeability are explored. Only two of the possible combinations of length scales and permeability relations provide a maximum value within the mush that can be chosen as a representative value for the given conditions. It is found that the Rayleigh number that uses the ratio of thermal diffusivity to the casting speed as a length scale provides the best separation between freckled and nonfreckled data. Critical values for the Rayleigh number are in the range of 38 to 46 for vertically solidified Pb-Sn and within the range of 30 to 33 for Ni-base superalloys. Although not exactly the same, the proximity of these intervals indicates that the critical Rayleigh number is not very sensitive to alloy-specific system parameters. The influence of sample pulling inclination angle on this critical value is assessed for Ni-base superalloys. A preliminary relationship between the critical Rayleigh number and the inclination angle is developed.

I. INTRODUCTION

FOR unidirectional solidification of castings, where the objective is to obtain a columnar structure, the presence of chains of small equiaxed grains (*i.e.*, freckles) is to be avoided. This concern is of chief importance for directionally solidified superalloy single-crystal parts, where the presence of freckles renders the part defective. For Pb-Sn alloys, there is admittedly no concern over the practical implications of the presence of freckles; however, simple binary alloys such as Pb-Sn are popular with experimental researchers because they provide insight into the same complicated phenomena that would be expected in more complex systems.

During upward directional solidification, the interdendritic liquid in the mushy zone is held by the frictional forces stemming from the presence of the dendrite arms, which essentially act as a solid boundary. However, due to microsegregation, light alloy elements will be rejected into the melt if the partition ratio is less than unity, or heavy elements will preferentially be incorporated into the solid, for partition ratios larger than unity. Under either of these two circumstances, the density of the liquid decreases and in some circumstances it may do so by a factor large enough so that the induced buoyant forces overcome the frictional resistance offered by the dendrites. At this point, a plume of liquid flows to upper regions causing remelting of the solid. This has as a consequence the formation of liquid channels within the mushy zone. This plume flow may tear off higher order dendrite arms and transport them elsewhere in the melt, where they might survive and form equiaxed grains. If the grains remain in the channel, they are later observed as freckles.

J.C. RAMIREZ, Graduate Research Assistant, and C. BECKERMANN, Professor, are both with the Department of Mechanical and Industrial Engineering, The University of Iowa, Iowa City, IA 52242. Contact e-mail: becker@engineering.uiowa.edu

Manuscript submitted May 14, 2002.

Numerical solutions of the full conservation equations to model freckle formation have been performed,[1,2,3] but the inherent complications of solving three-dimensional convection problems and computing the solidification path for multicomponent alloys have kept research in this area rather slow. Until software having the capability of effectively computing freckle formation is available, the casting industry has to rely on simplified criteria backed by experimental data.

Since freckle formation is due to the interaction of buoyancy and frictional forces, the Rayleigh number is the dimensionless parameter of choice to characterize this phenomenon. Rayleigh-number-based criteria are expressed in terms of a critical value. If the Rayleigh number for a given set of conditions is below a critical value, then freckles are not expected to form. The most complete work in this field is due to Worster.[4] Beckermann *et al.*[5] obtained a critical value for the Rayleigh number based on the experimental data of Pollock and Murphy[6] and then used numerical simulations to confirm their finding. Through additional simulations of inclined castings, they found that the critical Rayleigh number decreases with increasing inclination from the vertical. Auburtin *et al.*[7] have performed experiments on several commercial Ni-base superalloys and studied the influence of the inclination of the directionally solidified castings on the onset of freckling in terms of a critical Rayleigh number that is unique to each of the superalloys. Although the work of Auburtin *et al.* shows clear separation between freckled and nonfreckled samples, they evaluate the density inversion based on the liquid composition after freckles form. It should be noted, however, that a critical Rayleigh number must be based on the undisturbed, freckle-less state.

Several definitions of the Rayleigh number are available in the literature.[4–10] Even though they are all based on the notion of providing an indication of the interplay between frictional and buoyant forces, these definitions can vary significantly from researcher to researcher. The main areas

of discrepancy are the characteristic length scale and the choice of relationship that describes the permeability of the mushy zone. The typical length scales used are the mushy zone height, the primary dendite arm spacing and the ratio of the thermal diffusivity to the casting speed. Recently, Yang *et al.*[8] evaluated six different definitions and applied them all to the same set of data for the Pb-Sn and Pb-Sb systems. They found that some definitions work better than others do. They also showed that a strong correlation exists between their own definition of the Rayleigh number and the primary dendrite arm spacing, a finding that relates to that of Pollock and Murphy,[6] where a relationship between freckling and dendrite arm spacing is presented.

The objective of this study is to evaluate different Rayleigh-number-based criteria in terms of available experimental data for both Pb-Sn alloys and Ni-base superalloys. A critical value that represents the conditions below which freckles will not form is presented, and the influence of the casting inclination on this critical value is explored, for Ni-base castings. It should be pointed out, however, that the Rayleigh number is not the sole dimensionless parameter that would characterize an instability problem such as that presented by the formation of freckles. Indeed, in the stability analysis of Worster,[4] it is shown that the critical Rayleigh number varies with at least four other system parameters. These are the Stefan number, a dimensionless melt superheat, a parameter that describes the variation of the permeability with the solid volume fraction, and a ratio that characterizes the phase diagram. It would be unreasonable, therefore, to expect a universally valid value for the critical Rayleigh number applicable to Pb-Sn alloys, Ni-base superalloys, and all casting conditions. What should be expected from a study of available literature reporting experimental results is a freckle predictor criterion that naturally would depend on the alloy system and be applicable to the conditions explored in the experiments. To the authors' knowledge, this study represents the first time that a Rayleigh-number-based criterion is examined for both Pb-Sn and Ni-base superalloys. Such a criterion can be considered to be successful if it clearly predicts the conditions for freckle formation, even if the critical number is different for each alloy system considered.

II. RAYLEIGH NUMBER

A. *Definition*

Figure 1 shows a schematic representation of the unidirectional solidification system considered here. The sole coordinate considered here is y, defined as positive in the direction of increasing solid fraction. The liquid-mush interface is located at $y = 0$. The term G denotes the externally imposed temperature gradient, and R denotes the casting speed.

The mushy-zone Rayleigh number calculated here, in its most general form, is that defined as[4]

$$\mathrm{R}a_L = \frac{\left(\frac{\Delta\rho}{\rho_0}\right) g\overline{K}L}{\alpha\nu} \qquad [1]$$

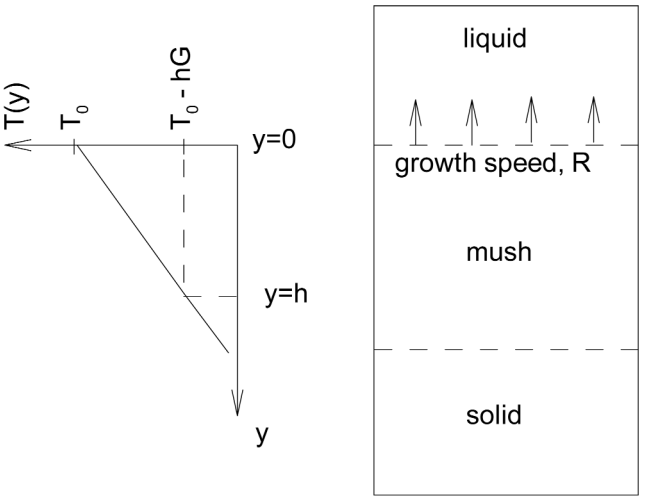

Fig. 1—Schematic representation of the unidirectional solidification system considered.

where L is a suitable length scale, α and ν are the thermal diffusivity and kinematic viscosity, respectively, g is the acceleration of gravity, $\Delta\rho/\rho_0 = (\rho_0 - \rho)/\rho_0$ is the relative density inversion over the mush height, ρ_0 is the density at the liquidus, and $\overline{K}$ is an average permeability. Properties like α and ν for Pb-Sn systems can be found in Table I, which is adapted from Reference 1. For all superalloys considered, the same approximate values of $\alpha\nu = 5 \times 10^{-12}$ m^4/s^2[5] and $\nu = 9.3 \times 10^{-7}$ m^2/s are used.

The values of the thermophysical properties presented in Table I for Pb-Sn alloys and those mentioned previously for Ni-base superalloys have uncertainties associated with them that must be acknowledged. Additionally, the assumption that these values are independent of the composition of the Pb-Sn alloys or the Ni-base superalloys introduces additional uncertainties. Even though these uncertainties are difficult to quantify, it would not be unreasonable to expect them to be ± 10 pct.

B. *Relative Density Inversion*

For Pb-Sn alloys, the density inversion can be calculated with

$$\left(\frac{\Delta\rho}{\rho_0}\right) = \beta_T (T - T_0) + \beta_C (C_l - C_0) \qquad [2]$$

where β_T and β_c are the thermal and solutal expansion coefficients. Here, the thermophysical properties of the Pb-Sn system were taken as constants, regardless of Sn concentration. The actual values used can be found in Table I. In Eq. [2], T_0 is the liquidus temperature corresponding to the initial Sn concentration, C_0, and it is obtained from the equilibrium phase diagram. In Eq. [2], T is the temperature distribution within the mush and it varies linearly from T_0 for $y = 0$ to $T_0 - hG$ for $y = h$. The term C_l is the Sn concentration distribution in the liquid within the mush and it is assumed to vary with T as follows:

$$C_l = C_e \left(\frac{T - T_m}{T_e - T_m}\right) \qquad [3]$$

Table I. Properties of Pb-Sn Alloys, Adapted from Reference 1

Property	Unit	Value
k		0.31
T_m	K	600
m	K/(wt pct)	−2.33
β_T	K^{-1}	$1.2 \cdot 10^{-4}$
β_c	$(\text{wt pct})^{-1}$	0.00515
v	m^2/s	$2.47 \cdot 10^{-7}$
α	m^2/s	$1.1 \cdot 10^{-5}$
T_e	K	456
C_e	wt pct	61.9

This relation is based on the assumption that the liquidus line in the equilibrium phase diagram is linear. In Eq. [3], T_m is the melting point of pure Pb, and T_e and C_e are the eutectic temperature and concentration, respectively, for the Pb-Sn system.

For Ni-base superalloys, the computation of the liquid density inversion for use with Eq. [1] is somewhat more complicated than for the Pb-Sn binary system. This involves the use of a multicomponent phase equilibrium subroutine developed by Boettinger *et al.*[11] that considers temperature and concentration dependence of partition ratios and liquidus slopes. A detailed explanation of the method can be found in Beckermann *et al.*[5] and Schneider *et al.*[12]

As in Section A, some sources of uncertainty can be identified in the calculation of the density inversion. For Pb-Sn alloys, the assumption of a straight liquidus line and constant values for the expansion coefficients undoubtedly will introduce uncertainty in the calculations. Although they are difficult to quantify, these uncertainties should be ±10 pct. For the Ni-base superalloys, the phase equilibrium subroutine of Boettinger *et al.*[11] and the method used to calculate the liquid densities also introduce uncertainties that should be ±10 pct.

C. *Solid Fraction*

Calculation of the solid fraction is necessary because the average permeability, $\overline{K}$, as will be stated in more detail subsequently, is a function of both the primary dendrite arm spacing and a mush-height averaged value of the solid fraction.

For Pb-Sn alloys, the local solid fraction, ε_s, is calculated *via* the Scheil equation:

$$\varepsilon_s = 1 - \left(\frac{C_l}{C_0}\right)^{\frac{1}{k-1}} \qquad [4]$$

where k is the partition coefficient. The value of k used can be found in Table I. For superalloys, a standard Scheil analysis together with the phase equilibrium subroutine by Boettinger *et al.*[11] is used.[5,12]

Estimates of the solid fraction from the Scheil analysis have some uncertainty. For the low solid fractions of interest here (<20 pct), these uncertainties can be assumed to be small. Furthermore, the same analysis is applied in all cases, implying that any uncertainty would be of a systematic nature and have little effect on the evaluation of the freckle criterion.

D. *Length Scale and Permeability Relations*

In the work of Beckermann *et al.*,[5] the permeability relation adopted was based on the isotropic Blake–Kozeny equation; *i.e.*,

$$\overline{K} = 6 \cdot 10^{-4} \cdot \lambda_1^2 \cdot \frac{\left(1 - \overline{\varepsilon}_s\right)^3}{\overline{\varepsilon}_s^2} \qquad [5]$$

where λ_1 is the primary dendrite arm spacing and $\overline{\varepsilon}_s$ is the mush height averaged, or mean solid fraction, given by

$$\overline{\varepsilon}_s = \frac{1}{h} \int_0^h \varepsilon_s \, dy \qquad [6]$$

The use of the mean solid fraction in Eq. [5] was first proposed by Worster[4] and is an attempt to model the average permeability over the mushy zone height without directly averaging the local permeability. Additionally, Beckermann *et al.*[5] used h (the distance from the mush-liquid interface) as the length scale in Eq. [1]; *i.e.*,

$$L = h \qquad [7]$$

Using Eqs. [5] and [7], Beckermann *et al.*[5] found that the resulting Rayleigh number successfully separates freckled and nonfreckled samples for the experiments of Pollock and Murphy[6]. Rayleigh number definitions that use Eq. [7] are denoted by Ra_h in the following.

Recently, Yang *et al.*[8] used a Rayleigh-number-based freckle predictor based on the ratio of the thermal diffusivity to the casting speed as the length scale; *i.e.*,

$$L = \alpha/R \qquad [8]$$

as suggested by Worster.[4] They found that their criterion performs remarkably well for Pb-Sn samples. Rayleigh number definitions that use Eq. [8] are denoted by $\text{Ra}_{\alpha/R}$ in the following.

The behavior of the Rayleigh-number-based on both length scales is examined in Figures 2 and 3. The two figures show the variation of the various Rayleigh numbers with average solid fraction for representative Pb-Sn and Ni-base alloys, respectively. The dash-dot-dot lines correspond to Ra_h and the Blake–Kozeny equation (Eq. [5]) for the permeability, *i.e.*, the original definition used by Beckermann *et al.*[5] Note the presence of a maximum around $\overline{\varepsilon}_s = 0.06$ in Figure 3. In Figure 2, the maximum appears to be at $\overline{\varepsilon}_s = 0$, but actually, the dash-dot-dot line starts from zero and increases very quickly. This feature cannot be discerned in the figure because of the scale. Hence, for the Pb-Sn alloys, the maximum in Ra_h is very close to the mush-liquid interface ($y = 0$), whereas for Ni-base superalloys, it is a little further inside the mush, as already noted in Reference 5. In any case, this maximum serves as a convenient and physically meaningful reference value of Ra_h for judging stability to freckle formation in both alloys.

The short-dash line in Figures 2 and 3 represents $\text{Ra}_{\alpha/R}$ and the permeability calculated again with the Blake–Kozeny equation. Note the lack of a representative value since $\text{Ra}_{\alpha/R}$ tends to infinity as $\overline{\varepsilon}_s \to 0$. Therefore, this definition was not considered further.

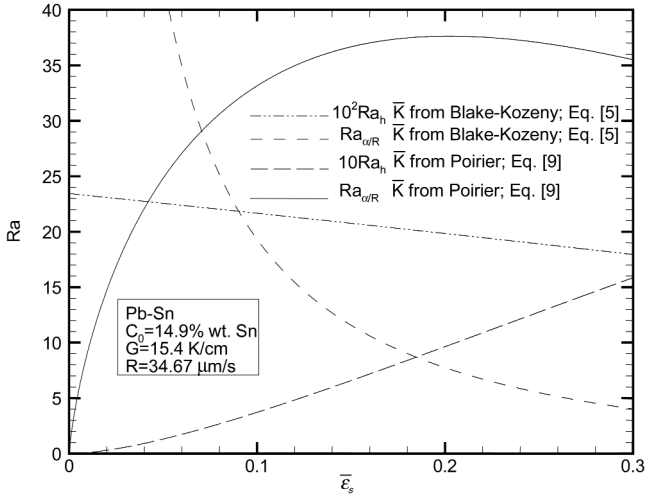

Fig. 2—Local variation of Rayleigh numbers for Pb-Sn defined in terms of different length scales and permeability relations.

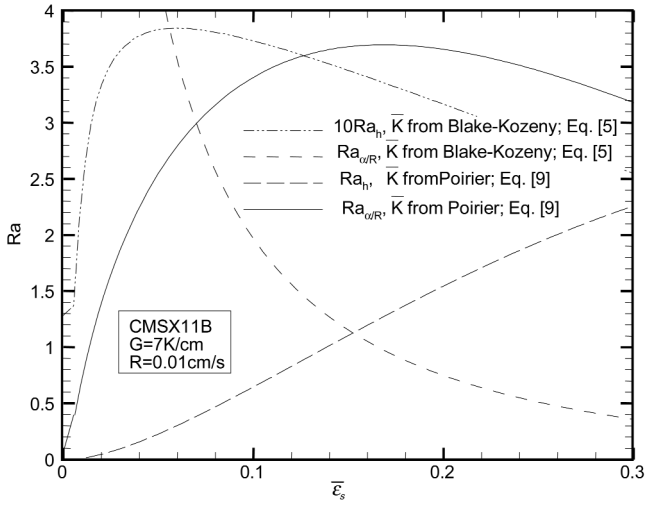

Fig. 3—Local variation of Rayleigh numbers for the CMSX11B superalloy defined in terms of different length scales and different permeability relations.

The reason Yang *et al.*[8] were able to use α/R as the length scale in the Rayleigh number and still observe a maximum in the mush is that they used a permeability relation that is different from the Blake–Kozeny equation. The use of a different permeability relation is therefore explored in the following. Felicelli *et al.*[2] propose an expression for the local permeability in terms of the local solid fraction in the direction parallel to the primary dendrite arms, and another one in the perpendicular direction. There is no clear physical reason that would support choosing one direction over the other. In this study, the parallel direction is chosen solely for simplicity. Because the functional form of the two permeability relations is similar, using the perpendicular direction would have yielded the same qualitative behavior. Yang *et al.* suggest taking the harmonic mean of the local permeability over the mush in order to obtain an average value. That approach was considered for the present work; however, it was found that directly evaluating the relation in Felicelli *et al.* at the average solid fraction yields an average permeability that exhibits the same general behavior as that obtained by taking the harmonic mean. Therefore, for the average permeability, the following expression is used:

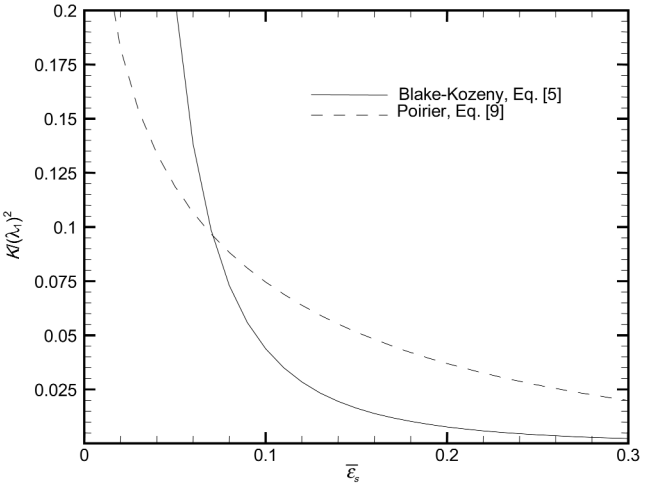

Fig. 4—Comparison of permeability relations. Solid line represents the Blake–Kozeny equation, given by Eq. [5]. The dashedl line is Poirier's equation, given by Eq. [9].

$$\overline{K} = 0.074 \cdot \lambda_1^2 \cdot \left(-\ln\left(\overline{\varepsilon}_s\right) - 1.49 + 2 \cdot \overline{\varepsilon}_s - 0.5 \cdot \overline{\varepsilon}_s^2\right) \quad [9]$$

which shall be referred to here as Poirier's equation. The solid lines in Figures 2 and 3 are constructed using Poirier's equation for the permeability in $Ra_{\alpha/R}$. It can be seen that there is indeed an easily identifiable maximum that can be used as a reference value for judging freckling stability. The maximum occurs at an average solid fraction between 0.15 and 0.2 for both Pb-Sn alloys and Ni-base superalloys. The behavior of Ra_h with Poirier's equation for the permeability was also considered, which is shown as long-dash lines in Figures 2 and 3. It is readily apparent that this definition does not provide an easily identifiable characteristic value. Note that both Eqs. [9] and [5] yield an infinitely large permeability for $\overline{\varepsilon}_s \to 0$, but Eq. [5] does so much faster. For illustrative purposes, these two permeability relations are compared graphically in Figure 4. The rapid increase in the permeability given by the Blake–Kozeny equation is compensated for, in Eq. [1], by the length scale h and the density inversion, both of which vanish for small solid fractions. The use of α/R as a length scale diminishes this compensating effect, as can be seen in Figures 2 and 3. On the other hand, the weaker rate of increase of permeability with decreasing solid fraction of Eq. [9] allows setting $L = \alpha/R$. In conclusion, if the length scale is chosen as h, then $\overline{K}$ should be calculated with the Blake–Kozeny equation, and if the length scale is chosen as α/R, then Poirier's equation should be used to calculate $\overline{K}$.

Uncertainties in the permeability are primarily due to uncertainties associated with the measurement or estimation of the primary dendrite arm spacing, λ_1. This is discussed in greater detail in Section III. Obviously, the use of either Eq. [5] or [9] will result in much different values of the permeability, for the same λ_1 and $\overline{\varepsilon}_s$. There is no information available in the literature that would allow for an uncertainty

assessment of either permeability relation. However, the basic premise is that the same permeability relation can be used for different alloys and casting conditions. Hence, any uncertainty in the permeability relation itself would be of a systematic nature and not affect the present evaluation of the freckle criterion. It should be kept in mind, however, that the use of different permeability relations (and length scales) results in different values of the critical Rayleigh number. This does not represent a problem since a universally accepted value of the critical Rayleigh number (for example, unity) does not exist.

III. EXPERIMENTAL DATA AND CALCULATIONS

A. *Pb-Sn Alloys*

Several researchers have carried out directional solidification experiments using Pb-Sn alloys, and the main results are shown in Table II, which is adopted from Yang *et al.*[8] and contains some other data not appearing in that study. The original reference is indicated in the table. The first column is the experiment number. The second column is the initial Sn concentration for the sample. The third column

Table II. Data for Pb-Sn Unidirectional Solidification Experiments

Experiment	C_0 (wt pct)	G (K/cm)	R (μm/s)	λ_1 (μm)	Data Group	Ra_h*	$Ra_{a/R}$**	Freckles?
1	33.4	75	8	166	A, Ref. 9	0.19	294	yes
2	34	17	30	172		0.95	85.7	yes
3	23.7	81	24	164		0.09	67.9	no
4	23.4	77	6	185		0.11	341.4	yes
5	27	59	64	155		0.14	25.9	no
6	30.3	20	6	208		0.94	559	yes
7	27.1	17	1	240		1.18	3993	yes
8	10	110	10	115		0.01	33.9	no
9	16.5	101	4	172		0.04	312	yes
10	57.9	105	10	234		0.82	811	no
11	54.7	67	40	177		0.66	110	no
12	2.5	12	11.75	300	B, Ref. 10	0.02	48.9	no
13	5	12	11.75	323		0.1	114	yes
14	10	12	11.75	293		0.34	187	yes
15	15	12	11.75	290		0.74	275	yes
16	20	10	11.75	330		2.06	474	yes
17	30	9	11.75	290		3.99	549	yes
18	40	7	11.75	290		9.12	732	yes
19	25	4	125	211†	C, Ref. 14	3.33	23	no
20	25	8	62.5	232†		2	55.04	yes
21	25	8	41.7	302†		2.44	140	yes
22	25	8	20.8	302†		3.4	281	yes
23	25	4	20.8	377†		10.6	438	yes
24	25	8	10.4	302†		3.4	562	yes
25	25	4	10.4	377†		10.6	876	yes
26	25	8	5.2	302†		3.4	1123	yes
27	14.9	15.4	34.67	185	D, Ref. 15	0.23	37.6	no
28	14.9	16.8	11.83	203		0.26	132	no
29	15.3	24.7	6.5	200		0.18	241	no
30	15.2	22.3	4	213		0.2	441	yes
31	14	34.2	2	208		0.12	775	yes
32	15	21.1	5.5	209		0.22	305	yes
33	20	1.5	47	206	E, Ref. 16	5.7	46.2	yes
34	20	1.5	130	172		3.75	11.6	yes
35	20	2.3	110	119		1.17	6.6	no
36	45	27.8	2	203†	F, Ref. 17	5.37	2370	yes
37	10	7.75	7.5	293	G, Ref. 18	0.52	293	yes
38	10	1.43	18.33	383		4.87	384	yes
39	10	2.73	6.39	401		2.79	644	yes
40	10	3.47	23.33	368		1.85	149	no
41	10	3.86	3.89	373		1.71	960	yes
42	10	4.54	26.67	329		1.13	104	no
43	10	5.18	3.06	374		1.28	1169	yes
44	10	3.63	33.33	342		1.53	90	no
45	10	4.64	16.67	355		1.29	193	yes

*Permeability calculated with Eq. [5].
**Permeability calculated with Eq. [9].
†Arm spacing estimated *via* Eq. [10].

shows the imposed temperature gradient and the next column shows the casting speed. Column 5 shows the primary dendrite arm spacing. Some of the references did not report values for the primary dendrite spacing. According to Klaren *et al.*,[13] given the temperature gradient G (in K/cm), and the casting velocity R (in μm/s), the primary dendrite arm spacing, in microns, for Pb-Sn alloys can be calculated as

$$\lambda_{1,\,\mathrm{Pb-Sn}} = \begin{cases} 588G^{-0.32} & ; R < 45\mu\mathrm{m/s} \\ \propto G^{-0.32}R^{-0.45} & ; R \geq 45\mu\mathrm{m/s} \end{cases} \quad [10]$$

The proportionality constant for large R was not given in Klaren *et al.*, but with the data provided therein, it is estimated to be, on average, 2900 with a standard deviation of 235. This estimated arm spacing was used only for those cases where the measured arm spacing was not reported, as indicated in Table II with a cross. Column 6 shows the name of the data group and the reference from which it was taken. Column 7 shows Ra_h (with $\overline{K}$ from the Blake–Kozeny equation) and column 8 shows $\mathrm{Ra}_{\alpha/R}$ (with $\overline{K}$ from Poirier's equation). The last column states whether freckles were encountered in the experiments.

The data shown in Table II correspond to laboratory-scale vertical directional solidification of cylindrical samples of a wide range of diameters and lengths.[8] Sample diameters varied from 5 to 38 mm. It should be pointed out that for larger sample diameters, the isotherms may not be completely flat due to lateral heat losses/gains. When the isotherms are concave (*i.e.*, with lower temperatures near the surface than in the center), the freckles will usually be located on the surface of the samples. Because not all the studies cited in Table II distinguish between freckles observed inside the sample and on the surface of the sample, such a distinction cannot be made here. All freckled samples are thus lumped together and vertical solidification with flat isotherms is assumed. It should be pointed out that inclined isotherms have a significant effect on the value of the critical Rayleigh number, as shown later. Therefore, the assumption of flat isotherms is a significant source of uncertainty. In the experiments of Table II, the thermal gradient G was measured. Because there is often no information in the original references regarding the measurement procedures or experimental uncertainties, it will be assumed that the uncertainty in G for all experiments is ± 10 pct. Sample lengths in the experiments ranged from 50 to 140 mm. These differences in lengths might affect the validity of the steady-state assumption for the casting speed, so there are also uncertainties associated with R. Since the growth speed is an externally imposed parameter controlled by the casting equipment, a conservative estimate for the uncertainty in R is ± 5 pct. The primary arm spacing values listed in Table II are those reported by the original researchers, unless otherwise indicated. Again, the studies often lack an uncertainty analysis for λ_1 and an uncertainty in λ_1 of ± 10 pct is assumed here.

B. *Ni-Base Superalloys*

The superalloy data for this study is that of Pollock and Murphy,[6] which can be found in Table III, and that of Auburtin *et al.*,[7] which is summarized in Table IV. The data in Table III correspond to experiments that were performed in a laboratory scale Bridgman furnace and in a production scale furnace capable of casting multiple blade shaped, rectangular slabs and cylindrical rods simultaneously. The samples cast in the laboratory scale furnace were cylindrical bars, measuring 13 mm in diameter and approximately 115 mm in length.[6] One data point in Table III represents a single experiment but may represent many samples due to the cluster casting capability. The data in Table IV are the results of experiments conducted in a custom-built vacuum induction furnace capable of casting a single sample at an angle with respect to the vertical orientation. All samples were cylindrical rods with a diameter of 25 mm and length of 150 mm.[7] For the reason discussed in Section B, flat isotherms are assumed for the data in both Tables III and IV. However, it should be kept in mind that this assumption is likely to be less accurate for the data in Table III that correspond to the production scale furnace with multiple samples.

In all, data for six different superalloys are available. Not all of the superalloys cast by Auburtin *et al.*[7] were considered in this study. In particular, the IN-718 samples were not used because this alloy contains 18 pct Fe; Fe is unfortunately not considered in the thermodynamic database linked to the subroutine of Boettinger *et al.*[11]

The primary dendrite arm spacing for the superalloys considered is estimated with[5]

$$\lambda_{1,\mathrm{Ni-base}} = 147\,(G \cdot R)^{-0.3384} \quad [11]$$

where G and R are in units such that the product of the two is in K/s yielding λ_1 in microns.

Tables III and IV provide the Rayleigh numbers Ra_h (with $\overline{K}$ from the Blake–Kozeny equation) and $\mathrm{Ra}_{\alpha/R}$ (with the permeability estimated *via* Porier's equation) for the two groups of Ni-base superalloy data. In Table IV, the first column indicates the type of alloy used in the experiment, the next two columns are the experiment number and the angle with respect to the vertical used for the unidirectional solidification of the sample. Auburtin *et al.*[7] presented temperature gradients at the liquidus (denoted in their article by G_{liq}) and the gradient at 50 pct solid fraction (which they denote as $G_{0.5}$). These temperature gradients were not experimentally measured but rather calculated with commercial casting simulation software. In this study, only G_{liq} was used for computing both the mushy zone depth and the primary dendrite arm spacing. The reason for this lies in the fact that where channels form the solid fraction is quite low (less than 20 pct) so the gradient at the liquidus is a reasonable approximation.

Regarding the data of Table III, the withdrawal rate R is externally imposed while the temperature gradient G is determined with one of the two following ways: For some samples, the thermal gradient was calculated by dividing the measured average cooling rate during solidification by the casting speed. For other samples, the gradient is "back calculated" by the use of empirical relationships between G, R, and λ_1, with measured values of the primary dendrite arm spacing. The original Reference 6 lacks a discussion of the experimental uncertainties associated with the measurements. As previously mentioned, the temperature gradient for the data in Table IV is obtained with simulation software, which should be quite accurate, yet some uncertainty could be associated with those estimates. As in Table III, the casting speeds listed in Table IV are values of an externally imposed

Table III. Data for Unidirectional Solidification Experiments of the SX-1 Superalloy from Pollock and Murphy[6]

Experiment	R (μm/s)	G (K/cm)	λ_1 (μm)	Ra_h*	$Ra_{\alpha/R}$**	Freckles?
1	4.2	78	467.4	0.13	281.1	no
2	4.2	73	478.0	0.15	294.05	no
3	14	96	289.9	0.04	32.45	no
4	14	81	307.1	0.05	36.4	no
5	56	23	294.1	0.18	8.34	yes
6	56	16.5	329.1	0.31	10.45	yes
7	56	12.9	357.7	0.47	12.35	yes
8	56	11	377.5	0.61	13.75	yes
9	56	7.7	425.9	1.1	17.5	yes
10	70	96.1	168.1	0.014	2.18	no
11	100	31.8	216.6	0.069	2.54	no
12	99	6	382.2	1.14	7.98	no
13	110	11	300.4	0.39	4.44	yes
14	113	10.8	299.5	0.39	4.29	no
15	113	10	307.4	0.44	4.52	yes
16	113	8.2	328.8	0.62	5.17	yes
17	127	7	333.4	0.75	4.73	no
18	176	60.5	143.9	0.016	0.64	no
19	176	56.2	147.5	0.018	0.67	no
20	4.2	75.5	472.6	0.139	287	no
21	14	89.2	297.2	0.047	34.1	no
22	56	9.8	392.6	0.74	14.9	yes
23	56	9.1	402.5	0.84	15.6	yes
24	56	7.2	435.7	1.24	18.32	yes
25	56	7	439.9	1.3	18.67	yes
26	56	6	463.5	1.7	20.73	yes
27	70	109	161.1	0.011	2	no
28	100	48.5	187.8	0.034	1.9	no
29	113	7.8	334.4	0.67	5.34	yes
30	113	6.9	348.6	0.83	5.82	yes
31	113	6	365.5	1.05	6.39	yes
32	113	5	388.7	1.42	7.22	yes

*Permeability calculated with Eq. [5].
**Permeability calculated with Eq. [9].

parameter set by the casting equipment in steady-state operation. Even though the uncertainty in this speed might not be as high as that associated with a directly measured quantity, it still should be considered. For the data in Tables III and IV, the dendrite arm spacing is calculated with Eq. [11], which has an uncertainty associated with it. As for the Pb-Sn alloys, the uncertainties in G, R, and λ_1 will be assumed to be ± 10, ± 5, and ± 10 pct respectively.

C. *Estimation of Uncertainties in the Maximum Rayleigh Number*

The effect of uncertainties on the maximum Rayleigh number calculated with Eq. [1] depends on the choice of the length scale. With $L = \alpha/R$, it is clear from Eq. [1] that $Ra_{\alpha/R}$ is independent of G, for a given value of λ_1. So, uncertainties in the thermal gradient have no effect on $Ra_{\alpha/R}$. From Eq. [1], it can be seen that $Ra_{\alpha/R}$ is inversely proportional to R, so an uncertainty in the casting speed of ± 5 pct will produce an uncertainty in $Ra_{\alpha/R}$ of ± 5 pct. When $L = h$, the Rayleigh number is inversely proportional to G and independent of R for a given value of λ_1. So, an uncertainty of ± 10 pct in G will produce an uncertainty in Ra_h of ± 10 pct. The measured primary arm spacing appears in Eq. [1] through the average permeability. The Rayleigh number is proportional to the square of the measured value of λ_1 for both the Blake–Kozeny equation and Poirier's equation. This means that an uncertainty of ± 10 pct in λ_1 will produce an uncertainty of ± 20 pct in Ra_h and $Ra_{\alpha/R}$. As was discussed in previous sections, there are additional uncertainties due to the use of constant thermophysical properties and simplifying assumptions such as straight liquidus lines and flat isotherms. The combined effect of all these uncertainties is a root-mean square average of the individual uncertainties. It is difficult to accurately assess the influence of all uncertainties on Eq. [1]. It can be stated, however, that it would be reasonable to expect the values of the Rayleigh number to have an uncertainty of about ± 20 pct. This estimate does not include the uncertainty associated with non-flat isotherms, especially for the data in Table III, and its magnitude could not be assessed. Auburtin *et al.*[7] do not provide a detailed uncertainty analysis but they do provide a general result stating that under the conditions of that study, the Rayleigh number as defined there can be calculated with a precision of ± 15 pct, which compares favorably to the estimate previously set forth here.

Table IV. Data for Unidirectional Solidification Experiments of Superalloys from Auburtin *et al.*[7]

Alloy	Experiment	θ	R (μm/s)	G_{lia} (K/cm)	λ_1 (μm)	Ra_b*	$Ra_{\alpha/R}$**	Freckles
CMSX 11B	1	0	17	23	440.3	0.17	32.2	no
(Cannon-Muskegon	2	0	17	23	440.3	0.17	32.2	no
Corp., Muskegon,	3	0	17	30	402.4	0.11	26.9	no
MI)	4	0	100	7	361.5	0.23	3.7	no
	5	20	17	23	440.3	0.17	32.2	yes
	6	20	100	7	361.5	0.24	3.7	no
	7	20	17	30	402.4	0.11	26.9	yes
	8	20	100	7	361.5	0.23	3.7	no
	9	35	17	23	440.3	0.17	32.2	yes
	10	35	100	7	361.5	0.24	3.7	no
	11	35	17	30	402.4	0.11	26.9	yes
	12	35	100	7	361.5	0.23	3.7	no
René 88	13	35	100	9	332.0	0.11	3.2	no
General Electric	14	35	17	26	422.4	0.09	30.6	yes
Aircraft Engines,	15	20	100	9	332.0	0.11	3.2	no
Fairfield, CT)	16	20	17	26	422.4	0.09	30.6	yes
	17	0	17	11	565.1	0.3	54.8	yes
Nim 80A	18	35	100	11	310.2	0.04	1.9	no
(INCO Alloys	19	35	17	26	422.4	0.04	21.1	yes
Intl., Huntington,	20	20	100	11	310.2	0.04	1.9	no
WV)	21	20	17	26	422.4	0.04	21.1	yes
	22	0	17	15	508.8	0.09	30.6	yes
Waspaloy	23	0	33	7	526.1	0.21	17.2	no
Pratt & Whitney,	24	0	32	23	355.4	0.04	8.1	no
East Hartford,	25	18	22	14	477.3	0.11	21.2	yes
CT)	26	25	20	14	492.9	0.12	24.9	yes
	27	34	50	11	392.3	0.09	6.3	no
	28	34	22	14	477.3	0.11	21.2	yes
	29	34	21	31	370.5	0.03	13.4	yes
Mar-M247	30	0	22	13	489.4	0.27	35.4	yes
(Martin-Marrietta	31	0	31	12	447.8	0.23	21	no
Corp., Baltimore,	32	18	22	13	489.4	0.26	35.4	yes
MD)	33	24	22	13	489.4	0.26	35.4	yes
	34	35	46	11	403.5	0.19	11.5	yes
	35	35	22	13	489.4	0.26	35.4	yes

*Permeability calculated with Eq. [5].
**Permeability calculated with Eq. [9].

IV. RESULTS AND DISCUSSION

A. *Pb-Sn Alloys*

Figures 5(a) and (b) are plots of the Rayleigh numbers for all Pb-Sn samples in each data group. Figure 5(a) is constructed using column 7 of Table II. Figure 5(b) uses column 8 of the same table.

For the Pb-Sn system, Figure 5(a) shows that the criterion with Ra_h and $\overline{K}$ from the Blake–Kozeny equation performs rather poorly; *i.e.*, there are too many data points for which Ra_h is low yet they presented freckles. On the other hand, Figure 5(b) shows a more clear separation between freckled and nonfreckled data within each group. It is not easily apparent that there would be a critical value of $Ra_{\alpha/R}$ that provides good separation across all the different groups. However, consider tentatively removing the sample with the lowest Rayleigh number (which corresponds to experiment 34, in group E with $Ra_{\alpha/R} = 11.6$), then a value of $Ra_{\alpha/R,crit} \approx 38$ provides a cutoff below which no freckled samples will be encountered for any data group. While there is some crossover (nonfreckled freckled samples with $Ra_{\alpha/R} \geq 38$), this is not too troubling because the critical Rayleigh number only establishes the point below which freckles will not form. The actual critical value could be anywhere between 38 and 46, since the lowest $Ra_{\alpha/R}$ for a freckled sample (not counting experiment 34) is 46.2, *i.e.*, experiment 33. Figure 5(b) is comparable qualitatively to the two lowermost plots in Figure 6 of Yang *et al.*,[8] which are referred to in that paper as the most reasonable of all the forms of the Rayleigh number examined there.

B. *Ni-Base Superalloys*

In Section A, it was shown that Ra_h fails for the Pb-Sn data, whereas $Ra_{\alpha/R}$ performs reasonably well. In this section, the two different criteria are applied to both sets of superalloy data available in order to assess their performance. Figures 6(a) and 6(b) show the Rayleigh numbers for the experiments of Pollock and Murphy[6] (summarized in Table III), and Figures 7(a) and (b) are for the data of Auburtin *et al.*[7] (Table IV). As before, the Blake–Kozeny equation is used for Ra_h and Poirier's equation is used for $Ra_{\alpha/R}$. Figure 6(a) shows that Ra_h provides excellent separation; *i.e.*, there are no freckled samples with low values of

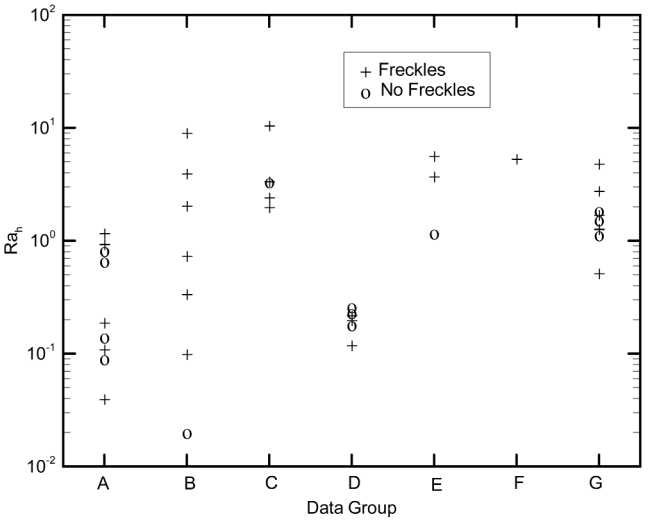

(*a*)

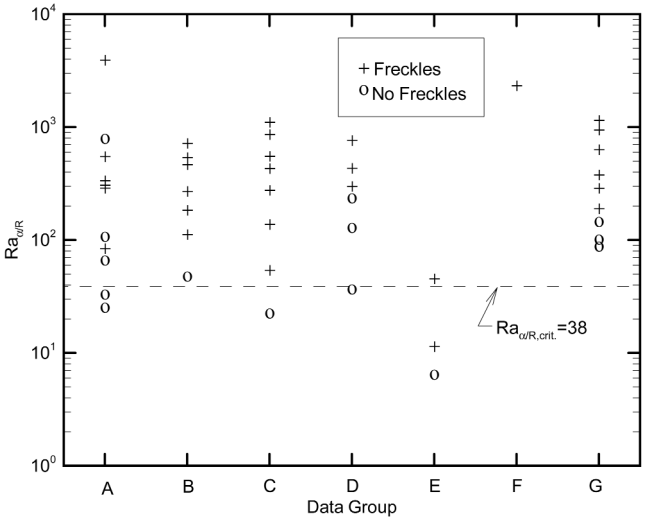

(*b*)

Fig. 5—(*a*)Rayleigh numbers based on *h* for Pb-Sn experiments listed in Table II. The permeability is obtained with Eq. [5]. (*b*) Rayleigh numbers based on α/R for Pb-Sn experiments listed in Table II. The permeability is obtained with Eq. [9].

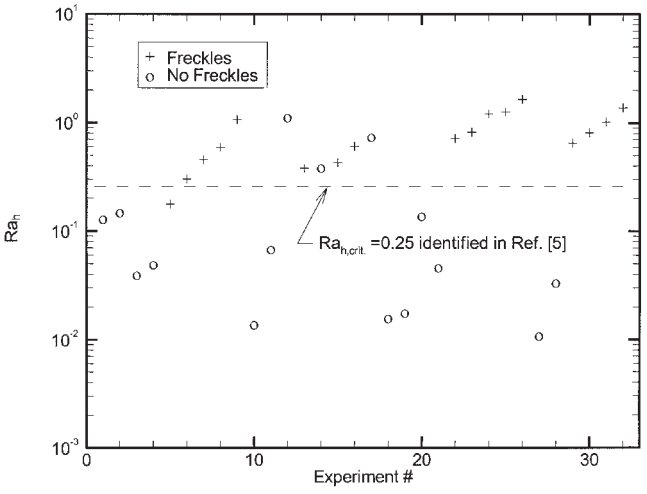

(*a*)

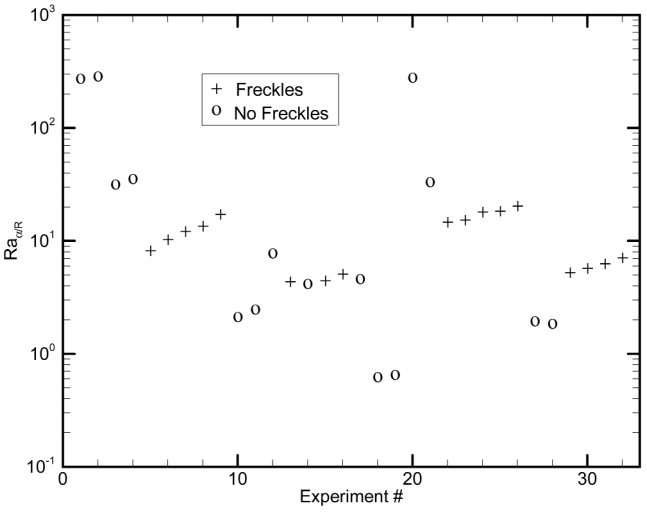

(*b*)

Fig. 6—(*a*) Rayleigh number based on *h* for experiments of Pollock and Murphy[6] (Table III). The permeability is obtained with Eq. [5]. (*b*) Rayleigh number based on α/R for experiments of Pollock and Murphy[6] (Table III). The permeability is obtained with Eq. [9].

Ra_h. This is why this definition was adopted in Beckermann *et al.*,[5] and a critical value of $Ra_h = 0.25$ was identified in that reference. Furthermore, inspection of Figure 6(b) reveals that $Ra_{\alpha/R}$ fails to effectively predict the formation of freckles for the data of Pollock and Murphy.[6] The reason for this is not clear, but it could be attributed to the fact that some of the data points in Table III represent experiments performed with multiple-sample clusters in a production scale furnace where inclination of isotherms is more probable.

So far, it has been shown that Ra_h with $\overline{K}$ from the Blake–Kozeny equation works well for the superalloy data of Pollock and Murphy[6] (as already shown by Beckermann *et al.*[5]), while failing for the Pb-Sn data. On the other hand, $Ra_{\alpha/R}$ with the permeability from Porier's equation fails for the superalloy data of Pollock and Murphy,[6] and succeeds reasonably well for the Pb-Sn data. The latter success is similar in nature to the results shown by Yang *et al.*,[8] even though they used a different permeability relation.

Figure 7(a) shows that Ra_h performs rather poorly with the superalloy data of Auburtin *et al.*[7] in Table IV, especially for larger inclinations. For zero inclination, if one could disregard the single freckled sample having a Ra_h of about 0.09, the critical value of 0.25 found for the Pollock and Murphy[6] data would actually work well, but this conclusion would be rather tentative because not enough data are available. In any case, the poor separation of the data at larger inclinations seems to disqualify Ra_h for this set of experiments.

Figure 7(b) shows the computed $Ra_{\alpha/R}$ for the superalloy data of Auburtin *et al.*[7] in Table IV. It can be seen that excellent results are obtained for the vertical samples as well as for the inclined castings. For 0 deg, the lowest value of $Ra_{\alpha/R}$ for a freckled sample is 30.6 (experiment 22, in Table IV) and the next point above it in Figure 7(b) has $Ra_{\alpha/R} = 32.2$ (experiments 1 and 2, in Table IV). The critical value then, for 0 deg, can be between 30 and 33, and is indicated in Figure 7(b) by a narrow band. This band en-

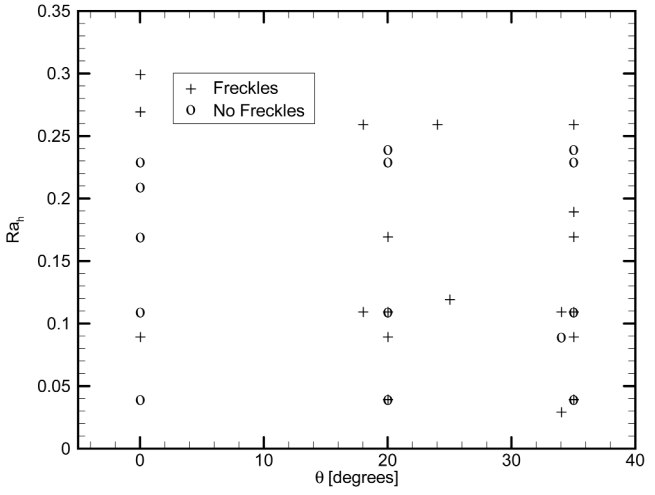

(*a*)

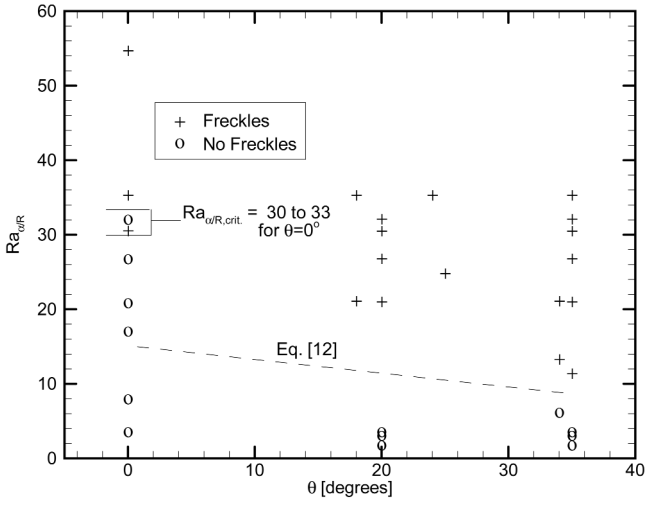

(*b*)

Fig. 7—(*a*) Rayleigh number based on *h vs* inclination angle with respect to the vertical for superalloys of experiments by Auburtin *et al.*[7] (Table IV). The permeability is obtained with Eq. [5]. (*b*) Rayleigh number based on α/R *vs* inclination angle with respect to the vertical for superalloys of experiments by Auburtin *et al.*[7] (Table IV). The permeability is obtained with Eq. [9].

compasses the small overlap exhibited by these data points and provides an estimate of a critical value for freckling. The small range of 30 to 33 indicates a variation that is well within experimental uncertainties and the approximations made in the estimation of material properties.

Note that this critical value for $Ra_{\alpha/R}$ of about 30 to 33 is rather close to the one established in the previous section for Pb-Sn alloys (*i.e.*, 38), both being for zero inclination. The difference could well be within the uncertainties of the experiments and calculations, such that a single critical value may be established for both types of alloys. On the other hand, the critical Rayleigh number is known to be a function of numerous other dimensionless parameters governing the system behavior, as discussed in Section I, and a single value for both the Pb-Sn and Ni-base superalloy systems cannot be expected.

It is well known that directional casting at an inclination angle with respect to the vertical orientation increases the chances of freckle formation.[5,7] When there is an inclination angle, low-density segregated liquid flows upwards inside the mush and accumulates along the upper sidewall. This accumulation occurs before channel formation and contributes to the initiation of an open channel. The larger the angle, the more segregated liquid will flow toward the upper sidewall, hence increasing the propensity of channel formation. In fact, in an inclined situation, all the available buoyancy contributes to advect the lighter fluid to the one location in the upper sidewall. Hence, even the smallest inclination augments channel formation propensity quite dramatically as observed in References 5 and 7. Two distinct approaches have been reported in the literature to incorporate the influence of the inclination angle on Rayleigh-number-based criteria. Auburtin *et al.*[7] proposes the introduction of a multiplication factor that involves the inclination angle and the permeability in the direction parallel and perpendicular to the dendrite arms. This requires introducing an additional empirical equation for the secondary dendrite arm spacing. Through the use of this multiplication factor, Auburtin *et al.* are able to keep their critical Rayleigh number around unity, regardless of inclination angle. On the other hand, Beckermann *et al.*[5] allow a variation of the critical Rayleigh number with inclination angle and develop a linear fit to describe this relationship. This latter approach will be adopted in the present work.

Beckermann *et al.*[5] showed that the slightest inclination causes a drop of approximately 50 pct in the critical Rayleigh number for no inclination. Hence, for angles slightly larger than 0 deg the critical value for $Ra_{\alpha/R}$ established previously would be reduced to about 15. Additionally, it can be determined from the numerical results of Beckermann *et al.* that for an angle of 35 deg, the critical Rayleigh number drops by about 40 pct with respect to the value for small inclinations. This means for the present system that the threshold value for 35 deg could be estimated at $Ra_{\alpha/R}$ (θ = 35 deg) = 9 (a 40 pct drop from 15). Note from Figure 7(b) that the value of 9 indeed provides good separation at 35 deg. Certainly, if more data were available for inclinations around 20 deg, a better observation could be drawn, but at least at first glance, linear interpolation (as in Reference 5) seems acceptable. This yields the following simple empirical relationship for the critical Rayleigh number:

$$Ra_{\alpha/R,\,\mathrm{crit}} = \begin{cases} 30 & ;\ \theta = 0 \text{ deg} \\ 15 - 0.172 \cdot \theta & ;\ \theta > 0 \text{ deg} \end{cases} \qquad [12]$$

which is plotted as a dashed line in Figure 7(b). Note that Eq. [12] was developed by assigning the same slope to the $Ra_{\alpha/R,\,\mathrm{crit}}$ (θ) line as in Beckermann *et al.*, even though in that reference, the slope was determined from the results of three computational experiments. The remarkable agreement between Eq. [12] and the experimental data shown in Figure 7(b) lends further support to the idea presented in Beckermann *et al.* that the decrease of the critical Rayleigh number with an increase in inclination angle can be predicted with a simple linear model. The sharp drop in critical Rayleigh number for small inclinations with respect to that for zero inclination reflects the fact discussed previously that these slightly inclined cases are much more prone to freckling than a noninclined case with all other casting parameters equal.

One important feature of Figure 7 must be pointed out. Note that the scale of the ordinate axis is not logarithmic as

in Figures 5 and 6. The separation of freckled and nonfreckled samples seen in Figures 5(b) and 6(a) would not be so clear had a linear scale been used. On the other hand, Figure 7(b) provides remarkable separation even with a linear scale on the ordinate axis for all inclinations. The success in using $Ra_{\alpha/R}$ as a freckle criterion for the Ni-base superalloy data of Auburtin *et al.*,[7] as well as to a reasonable extent for the Pb-Sn data, therefore constitutes the main finding of the present study.

Some discussion regarding the magnitude of the critical Rayleigh number obtained in the present study is appropriate. As pointed out by Auburtin *et al.*[7] the actual magnitude of the critical Rayleigh number varies significantly from one researcher to the next, with some reporting values of order unity and others finding critical Rayleigh numbers in the hundreds. Auburtin *et al.* adopt the idea presented by Sarazin and Hellawell[10] that the length scale should be of the same order of magnitude as the primary arm spacing in order to obtain a critical value of the Rayleigh number of order unity. It seems, however, that the length scale should be chosen as in Worster[4] so that the Rayleigh number obtained has some physical meaning. Furthermore, the Rayleigh number need not be unity to indicate propensity to channel formation. In fact, Worster's stability analysis[4] reports that for an aqueous solution of ammonium chloride, chimneys will appear when his definition of the Rayleigh number exceeds a value of about 150. Furthermore, Figure 4 shows that at low solid fraction, two accepted correlations yield values for the permeability that can be significantly different in magnitude from each other, so picking one correlation over the other will in turn yield vastly different values of the Rayleigh number. As long as the same equation for permeability is used across a wide range of data for consistency, the actual numerical critical value is unimportant. In fact, Yang *et al.*[8] report a critical value of 1 for their definition of the Rayleigh number by using a permeability relation proposed by Poirier in the late 1980s. If, however, another permeability relation is used (say, Eq. [9], also due to Poirier), the numerical values will be completely different, yet the predictive capability of the criterion will most probably be unaffected.

V. CONCLUSIONS

A criterion for predicting the formation of freckles for Pb-Sn and Ni-base superalloys has been evaluated. The criterion is based on a maximum value of the Rayleigh number, which indicates that the magnitude of buoyancy forces is largest with respect to the retarding frictional forces. The definition of the Rayleigh number involves a characteristic length scale. The two options explored in this study were the distance from the liquid mush interface and the scale represented by α/R, *i.e.* the ratio of thermal diffusivity to the casting speed. Additionally, two alternative ways of computing the mushy zone permeability where explored. Only two of the possible combinations of length scales and permeability relations provide a maximum value within the mush that can be chosen as a representative value for the given conditions.

It was found that $Ra_{\alpha/R}$ provides reasonable prediction of the formation of freckles for the widest array of data. The data include both Pb-Sn alloys and Ni-base superalloys and represent 80 experiments from 8 different sources. Only for the Ni-base superalloy data of Pollock and Murphy[6] does Ra_h perform better than $Ra_{\alpha/R}$.

A critical value of $Ra_{\alpha/R}$ in the range of 38 to 46 is suggested for vertically solidified Pb-Sn alloys and within the range of 30 to 33 for Ni-base superalloys. The proximity of these intervals indicates that the influence of other system parameters[4] on the critical Rayleigh number is not very strong. In fact, the difference could be within the uncertainty of calculating the Rayleigh number. Performing additional experiments with both alloy systems and carefully documenting experimental and property estimation uncertainties is recommended. Also, gathering data on a third alloy system, say, a transparent alloy, and evaluating the proposed criterion with that additional data set could provide additional insight into the influence of system parameters on the critical Rayleigh number.

The influence of sample inclination angle on the critical value was assessed for Ni-base superalloys. When the inclination increases to around 35 deg with respect to the vertical, the critical Rayleigh number drops to approximately 9. A relationship between the critical Rayleigh number and the inclination angle is developed. The concept behind Eq. [12] that the critical Rayleigh number decreases linearly with increasing inclination was first presented in Beckermann *et al.*[5] and was based on computer simulations. Here, it has been given some experimental support. Equation [12] should be refined further with more experimental data, especially with points for inclination angles smaller than 20 deg. Therefore, caution is recommended when using this equation.

When applying the proposed Rayleigh number criteria, it is recommended to keep in mind that exceeding the critical number does not imply formation of freckles, but rather that the conditions for such phenomena are favorable. For example, as pointed out in, Reference 5, the cross-sectional area of a casting might be too small to support the flow patterns associated with freckle formation, so even though the Rayleigh number might be larger than the critical value, freckles will not form. The same is true for castings of insufficient height.

ACKNOWLEDGMENTS

This work was supported, in part, by NASA under Contract No. NCC8-199. The authors thank Professors S. Cockcroft, S. Tewari, and T. Pollock for providing data and fruitful discussions.

REFERENCES

1. J. Guo: Ph.D. Thesis, The University of Iowa, Iowa City, IA, 2000.
2. S.D. Felicelli, D.R. Poirier, and J.C. Heinrich: *Metall. Mater. Trans. B*, 1998, vol. 29B, pp. 847-55.
3. M.C. Schneider and C. Beckermann: *Metall. Mater. Trans. A*, 1995, vol. 26A, pp. 2373-88.
4. M.G. Worster: *Ann. Rev. Fluid Mech.*, 1997, vol 29, pp. 91-122.
5. C. Beckermann, J.P. Gu, and W.J. Boettinger: *Metall. Mater. Trans. A*, 2000, vol. 31A, pp. 2545-57.
6. T.M. Pollock and W.H. Murphy: *Metall. Mater. Trans. A*, 1996, vol. 27A, pp. 1081-94.
7. P. Auburtin, T. Wang, S.L. Cockcroft, and A. Mitchell: *Metall. Mater. Trans. B*, 2000, vol. 31B, pp. 801-11.
8. W. Yang, W. Chen, K.M. Chang, S. Mannan, and J. deBarbadillo: *Metall. Mater. Trans. A*, 2001, vol. 32A, pp. 397-405.

9. S.N. Tewari and R. Shah: *Metall. Mater. Trans. A*, 1996, vol. 27A, pp. 1353-62.
10. J.R. Sarazin and A. Hellawell: *Metall. Trans. A*, 1988, vol. 19A, pp. 1861-71.
11. W.J. Boettinger, U.R. Kattner, S.R. Coriell, Y.A. Chang, and B.A. Mueller: in *Modeling of Casting, Welding and Advanced Solidification Processes VII*, M. Cross and J. Campbell, eds., TMS, Warrendale, PA, 1995, pp. 649-56.
12. M.C. Schneider, J.P. Gu, C. Beckermann, W.J. Boettinger, and U.R. Kattner: *Metall. Mater. Trans. A*, 1997, vol. 28A, pp. 1517-31.
13. C.M. Klaren, J.D. Verhoeven, and R. Trivedi: *Metall. Trans. A*, 1980, vol. 11A, pp. 1853-61.
14. M.I. Bergman, D.R. Fearn, J. Bloxham, and M.C. Shannon: *Metall. Mater. Trans. A*, 1997, vol. 28A, pp. 859-66.
15. L. Wang, V. Laxmanan, and J.F. Wallace: *Metall. Mater. Trans. A*, 1988, vol. 19A, pp. 2687-94
16. N. Streat and F. Weinberg: *Metall. Trans.*, 1974, vol. 5, pp. 2539-48.
17. R.N. Grugel and L.N. Brush: *JOM*, 1997, pp. 26-30.
18. J.R. Sarazin: Ph.D. Thesis, Michigan Technological University, Houghton, MI, 1990.